Analysis of the impact of different temporal aggregation techniques of land surface temperature on SUHI indicators and the relationship of surface temperature with population density and night lighting

Gawuc Lech[1]; Struzewska Joanna[1]

[1] *Politechnika Warszawska, Faculty of Environmental Engineering, Nowowiejska 20, Warsaw, Poland, lech.gawuc@is.pw.edu.pl*

dated : 1 July 2015

1. Introduction

The term "urban heat island" (UHI) typically refers to the difference between air temperatures observed in urban and rural areas. Voogt and Oke (2003) addressed methodological questions raised previously by Roth et al., (1989) and proposed the term "surface urban heat island" (SUHI). Despite complex interactions across scales, the physical coupling of surface and atmosphere makes identification of SUHI a logical path to identifying mitigations for UHI (Clinton & Gong, 2013). Using remote sensing to study SUHI can improve understanding of the spatial–temporal variability of physical processes which influence the long-term urban climate (Hu et al., 2013).

There have been significant efforts put into understanding the land surface temperature (LST) patterns over urban and rural areas (e.g. Carlson et al. 2000; Stathopoulou et al., 2007; Walawender et al., 2014; Zheng et al., 2014; Mohan et al., 2015). One of the most frequently investigated relationships that describe anthropogenic modification of natural surfaces is the relationship between impervious surface area (ISA) and surface temperature (e.g. Dousset et al., 2003; Yuan et al., 2007). However, Li et al., 2014 documented that LST is affected not only by land cover pattern but also by other anthropogenic forces. Thus, the linkage between anthropogenic heat flux (AHF) and surface temperature has been explored (Kato et al., 2005; Zhou et al., 2011). Also, indirectly described human activity or population characteristics and LST has also been extensively studied, e.g. population density (Buyantuyev et al., 2010; Mallick et al., 2012); socioeconomic patterns (Buyantuyev et al., 2010); human settlement characteristics including household income or population race (Jenerette et al., 2007). Remotely sensed night lights is another interesting parameter that has been used to spatially allocate many aspects of human activity (Gallo et al., 1995; Elvidge et al., 1997; Yang et al., 2014). Hence, since relationship between ISA, population density, night-time lights and surface temperature or human activity is well established, it is safe to anticipate that those variables can be used as spatial proxy of urban settlements, and therefore as a clue to delineate between urban and rural areas. However, little is known about the impact of temporal aggregation of LST data on the relationship between LST data and parameters describing human activity or surface properties. Filling this gap is one of the objectives of this study.

SUHI is a phenomenon not only of high spatial variability, but also of high temporal variability (Weng et al., 2014). Studies that investigate urban LST observed in different seasons frequently utilize a single satellite measurement and do not incorporate temporal composites (e.g. Sharma et al., 2014). Since surface temperature is influenced by accident synoptic conditions (e.g. wind, humidity), such approach may lead to discrepancies. In order to avoid such uncertainties it is advisable to use temporal composites. Analysis of long-term land surface temperature data composites is important in many aspects of urban climatology, i.e. seasonal and annual LST variability investigations, development of UHI mitigation strategies or composition of mean climatologies for modelling purposes. Composite data directly increase the clear sky coverage across urban and rural regions, which are beneficial for SUHI studies; however, many papers do not consider the possible errors caused by composite processes (Hu et al., 2013). Although previous investigations of MODIS multi-temporal urban LST patterns do account for cloud contamination (e.g. Cui et al., 2012; Hu et al., 2013; Quan et al., 2014), they fully or partially neglect spatial pattern of LST retrieval errors which may influence local and overall quality of resulting LST patterns and calculated SUHI intensities.

The primary objective of this paper is to estimate a mean intensity of SUHI phenomenon in Warsaw, Poland in the transitional seasons (Spring and Autumn) for the last 15 years by investigating the influence of temporal aggregation of LST data on several indicators of SUHI (Schwarz et al., 2011). According to the nature of remote sensing observations and typical cloudiness conditions in the target city, the idea of the approach was to promote those observations that represent the highest quality of LST retrieval. This was achieved by utilizing a weighted arithmetic mean, which weights were based on MODIS Quality Control (QC) metadata (Wan, 2006).

2. Study area

City of Warsaw has an area of 517.24 km^2. Population is about 1 700 000 inhabitants, but in the agglomeration it exceeds 2 500 000 persons. The average population density is 4223 persons/km^2. Warsaw is located in the

central part of Poland, at 78 to 121 m above sea level. Through Warsaw flows the biggest river in Poland, Vistula. According to the Climatological Atlas of Poland, the average annual number of cloudy days (more than 7 octanes) in the years 1971-2000 is between 140 and 150 (in winter 50-60 days), while the average annual number of cloudless days (less than 2 octanes) is between 30 and 40 (in winter 5 to 10 days). Since Warsaw has a transitional climate, synoptic conditions may be very different from year to year. In the north of Warsaw lies Zalew Zegrzyński Lake. Because of its proximity to the Warsaw agglomeration (about 10 km) and size (33 km^2) it was used as a reference to calculate one of the SUHI intensity indicators ("urban mean - water").

3. Data and methodology

Since transitional seasons (Spring and Autumn) in Poland, typically, have high variability of synoptic conditions, we utilized all available MODIS Terra MOD11A2 (V5) products that represent an average LST for 8 days from year 2000 to 2014. For each case analysed we chose 4 consecutive MOD11A2 products that corresponded with the Spring and Autumn Equinox (approx. 2 products before and 2 after). To sum up, there were 120 mean rasters for Spring case (day + night) and 120 for Autumn case (day + night), which cumulatively represent 1920 satellite acquisitions. MODIS Aqua observations were neglected due to different time of satellite overpass and unavailability of observations in the period 2000 - 2002. Moreover, in order to account for cloud contamination, we neglected those rasters with the number of available LST pixel lower than 50%. Also, unreliable LST values (lower than -15°C and more than 25°C) where neglected.

Night-time lights were collected by Suomi National Polar-orbiting Partnership Visible Infrared Imaging Radiometer Suite (Suomi NPP VIIRS). The "DNB Cloud Free Composites" product that was utilized has about 330 m spatial resolution and 14 bit radiometric resolution. The NPP VIIRS is a superior instrument to Defense Meteorological Satellite Program Operational Linescan System (DMSP OLI) since it has better technical characteristics (Elvidge et al., 2013). Particularly, NPP VIIRS product it not saturated over urban areas, while DMSP, due to low radiometric resolution (6 bit) is. Population density as a homogeneous shapefile was obtained from Geostat, (EOSTAT_Grid_POP_1K_2011_V1_0). Impervious surface area global raster was obtained from NOAA (Elvidge et al., 2007). Both rasters have resolution of 1 km.

3.1 Estimation of 15-year mean LST rasters

Each MOD11A2 product consist of 12 Scientific Data Sets (SDS). In this study we utilized SDSs that contained LST values, Quality Control and number of clear sky days in an 8-day period. The idea for the estimation of mean LST in the 15 year period was to promote those pixels that had the highest quality. Therefore, for each pixel that was taken into account, we applied weights based on values of LST retrieval errors (5 thresholds - Table 1) and number of clear-sky days (synonym of number of obtained observations during an 8 day period).

Description of LST retrieval errors	Weight value
good quality, not necessary to examine more detailed QC	5
average LST error <= 1K	4
average LST error <= 2K	3
average LST error <= 3K	2
average LST error > 3K	1

Table 1 Assignment of weight values based on MOD11A2 product Quality Control (MODIS User Guide - Wan, 2006).

Each pixel on each raster had appropriate weights applied and a final 15-year averaged LST image was built by means of weighted arithmetic mean. Weights were accumulated over all 8-day mean rasters from years 2000-2014 that were taken into account (60 per case). In order to broaden the analyses, we derived 3 types of final averaged rasters. Each was built by weighted arithmetic mean, where weights were of 3 different types. First type was based on LST retrieval errors, second was based on degree of cloudiness (number of clear-sky days), third was based on the sum of weights in first and second cases combined. Since the idea for estimating the final 15-year mean LST values was to promote pixels with the highest quality, we applied 5 exponential power to each weight. Consequently, the higher the exponential power applied, the stronger the promotion of highest quality pixels was. It was assumed that LST retrieval error is a final indicator of pixel quality and additional accounting for emissivity errors was neglected (Wan, 2006).

3.2 SUHI indicators

In order to quantify the impact of temporal aggregation and to estimate a mean SUHI intensity for the last 15 years in the city of Warsaw, we calculated several SUHI indicators that were used by various authors over those years. According to the remarks given by Schwarz et al., 2011, we used several indicators in parallel. Table 2 shows the list of indicators that were used, with a brief definition. For full descriptions please refer to Schwarz et al., 2011 and original papers. However, according to the specifics of this paper, some of the indicators had a slightly different definition or name than in the original references.

	Name	Brief definition
1.	Standard Deviation	Standard deviation of LST values within city's administrative borders

2.	Magnitude	Maximal LST – mean LST (within city borders)
3.	Range	Maximal LST – lowest LST (within city borders)
4.	Urban mean – other	Mean LST (within city borders) – mean LST (areas outside borders within a buffer)
5.	Urban mean – water	Mean LST (within city borders) – LST of Zalew Zegrzyński Lake
6.	Urban mean – agriculture	Mean LST (within city borders) – LST of cropland pixel
7.	Inside urban – inside rural	within city borders: mean LST of artificial areas – mean LST of natural areas
8.	Urban core – rural ring	mean LST of artificial areas within city borders – mean temperature in ring of pixels outside city
9.	Urban core – deep forest	mean LST of artificial areas within city borders – pixel covered with dense forest (Kampinos National Forest)

Table 2 SUHI indicators that were utilized.

4. Results

4.1 Spatial distribution of LST in different seasons

The aim of the study is to estimate an average SUHI intensity for the last 15 years. SUHI intensities are expressed as a number; however, according to the nature of temporal aggregation and the fact that surface temperature has a specific pattern in urban areas, it is advisable to initiate analyses with investigation of spatial distribution of LST. Such approach helps to avoid errors in the analyses. In order to achieve this goal, it was critical to select an appropriate way of LST temporal composites construction. We chose a combination of LST retrieval errors and clear-sky days weights for further analyses since it gave the most realistic spatial distribution pattern of urban LST and it fully exploits MODIS Quality Control metadata.

Figure 1 shows spatial distribution on 15-year mean rasters obtained for each case: Spring day, Spring night, Autumn day and Autumn night. Images were constructed using a sum of weights based on number of clear-sky days and LST retrieval errors. In each case there is the same trend observed - growing exponential power increases LST. Moreover, growing exponential power impacts the spatial range of elevated LST in Autumn day case and Spring night and day case - the bigger the power, the smaller the spatial range.

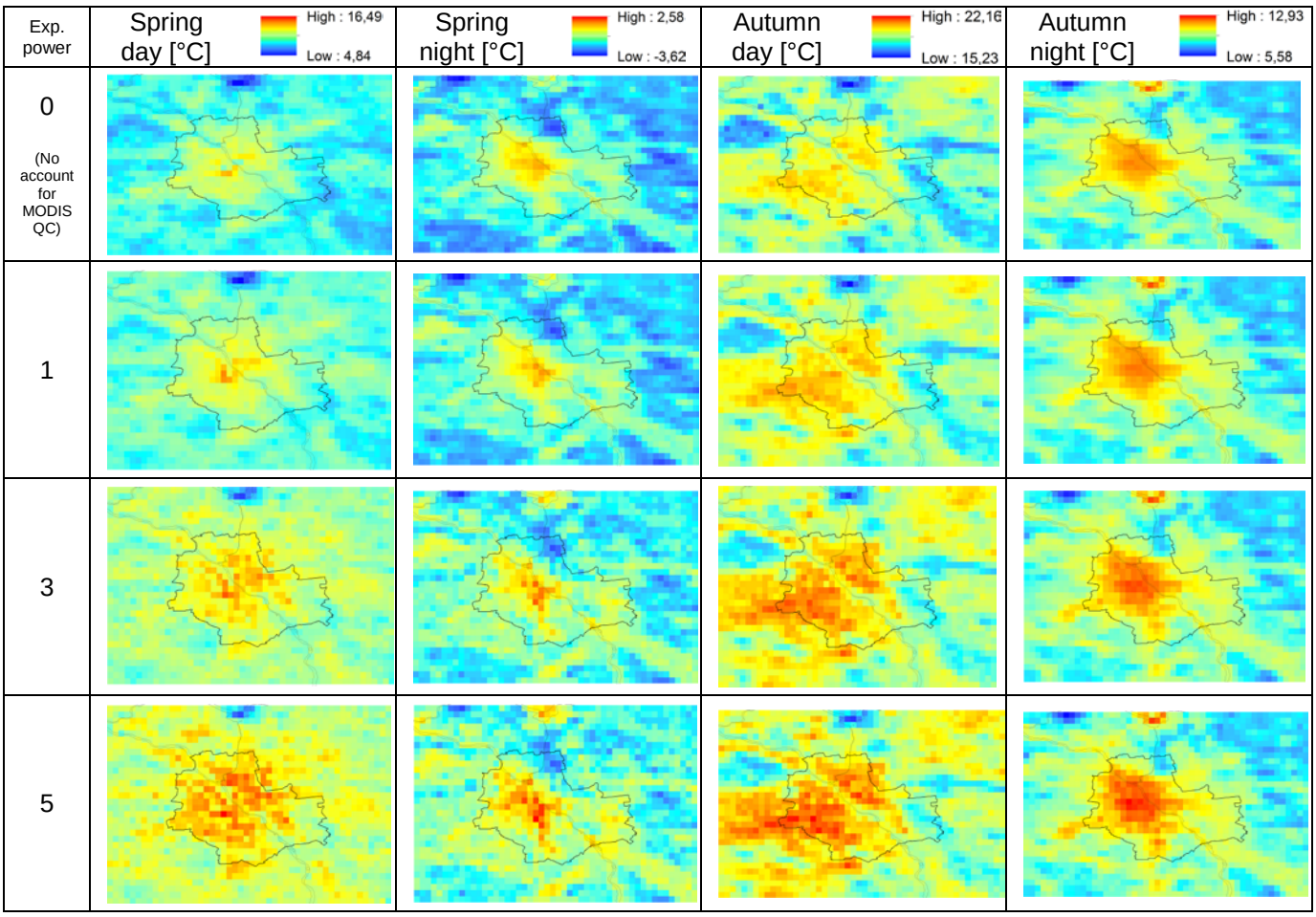

Fig.1 Spatial distribution of temporarily composited LST in different seasons.

On the other hand, growing exponential power has much less influence on spatial range of elevated LST in Autumn night case. The daytime and night-time cases show different spatial pattern of LST. In the night-time cases there is no river Vistula visible in the middle of the city, while during the daytime cases there is. This is

consistent with typical diurnal behaviour of LST in Warsaw (Gawuc, 2014). On the whole, in each case LST pattern seems plausible.

4.2 SUHI intensities

In order to underline the influence of MODIS Quality Control on temporal composite of LST, we calculated SUHI indicators values on 15-year mean rasters that were constructed by two types of arithmetic mean - simple (hereafter named "first" type of temporal aggregation composition process) and weighted arithmetic mean (hereafter named "second"). First type does not take into account MODIS QC and second does. Table 3 shows SUHI indicator values calculated on rasters that were constructed by means of a simple mean.

	[°C]	Autumn day	Autumn night	Spring day	Spring night
1.	**Standard Deviation**	0,89	0,97	1,15	0,83
2.	**Magnitude**	1,44	1,88	3,55	1,9
3.	**Range**	4,02	4,56	6,75	4,51
4.	**Urban mean - other**	0,81	1,49	1,5	1,15
5.	**Urban mean - water**	4,22	-1,71	5,93	-0,02
6.	**Urban mean - agriculture**	-0,03	1,4	1,64	1,05
7.	**Inside urban – inside rural**	1,04	1,28	1,57	1,01
8.	**Urban core – rural ring**	1,06	2,17	1,87	1,63
9.	**Urban core – deep forest**	3,04	1,45	4,21	0,6

Table 3 Indicator values calculated on rasters that were constructed by means of a simple mean.

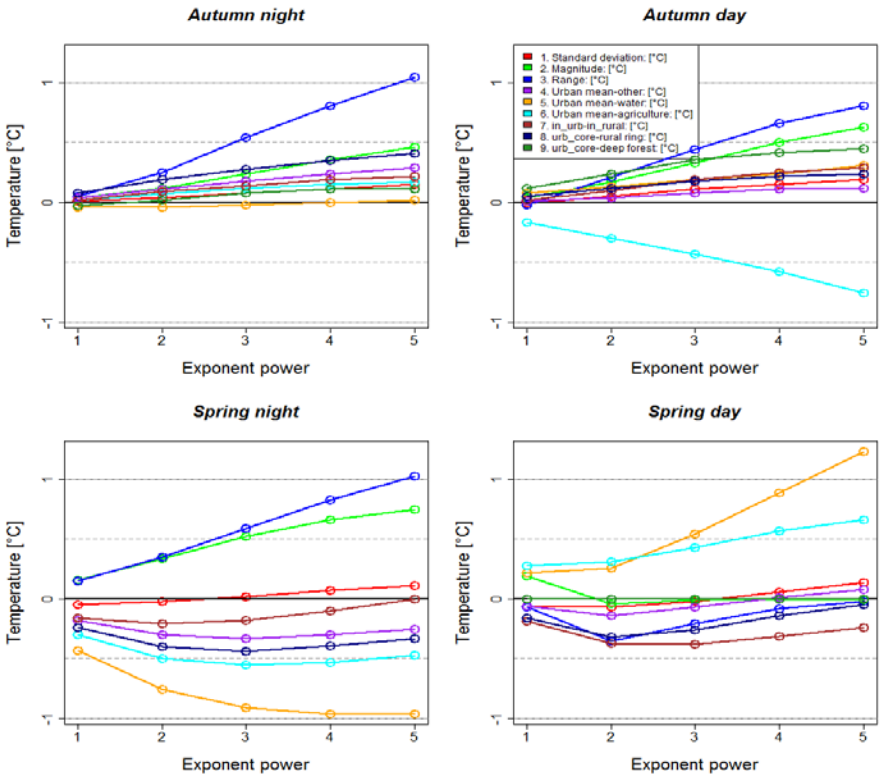

Fig. 2 SUHI indicator values - differences between two types of temporal composition.

In each case observed there is a clear trend visible – the higher the exponential power applied to weights, the bigger the difference between two types of compositions (Fig. 2). This clearly corresponds to the strength of promotion of pixels with best quality. Each indicator in Autumn cases calculated by means of the raster processed with the second type of temporal aggregation has a higher or almost the same value than after processing with the first type. This means that growing exponential power applied to weights during composition process causes higher contrasts in LST observed in urban and rural areas and directly increases SUHI intensity. The only exception is indicator "urban mean - agriculture", which is inversely proportional to growing exponential power. In Spring cases most indicators calculated on rasters built by two temporal aggregation processes have lower values after second type of composition, with the exception of indicators "range" and "magnitude" in night-time case and "urban mean - water" and "urban mean - agriculture" in daytime case. It is worth mentioning that the highest differences between two types of temporal composition processes are observed in Spring cases, which corresponds to high variability of synoptic conditions that can be observed throughout the 15 year period in this season and consequent low quality of satellite observations.

Summarizing, analysis of Table 3 and Fig. 2 leads to the conclusion that temporal composition process with regard to MODIS QC has a clear impact on calculated intensity of SUHI phenomena. In Autumn cases it mostly increases and in Spring cases it decreases SUHI intensity. However, some of the indicators show different

relationship with temporal aggregation processes, what seems to be consistent with findings of Schwarz et al. 2011, who documented rather low correlation between different SUHI indicators.

4.3 Relationship between aggregated LST and night-time lights, population density and ISA

Physical parameters that describe human activity or surface properties have an apparent pattern in urban areas. Typically, highest population density or night-time lights intensity and ISA values are observed in the city centres, which is an analogy with surface temperature. Therefore, variability of correlation throughout exponential powers reveals partially the impact of temporal aggregation process on LST pattern.

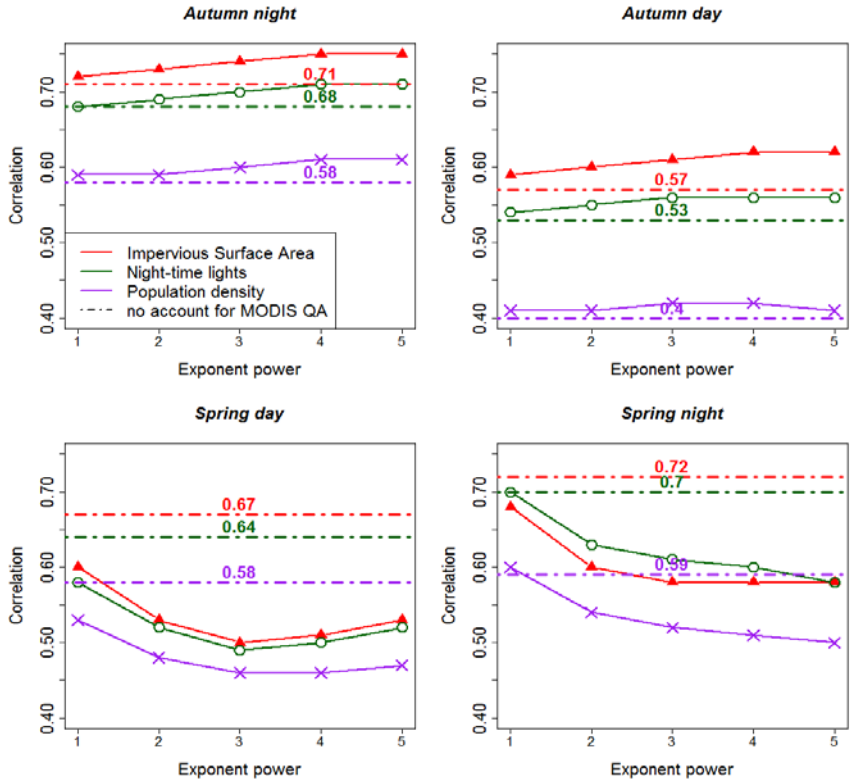

Fig. 3 Correlation coefficient variability across exponential power applied to weights.

Fig. 3 documents the impact of temporal aggregation of LST data on the relationship with night-time lights, population density and impervious surface areas. In each case the correlation coefficient was positive. In Autumn cases differences between first and second type of aggregation process (see Section 4.3) are not as apparent as in Spring cases. Moreover, in Autumn cases temporal composition process increases and in Spring cases temporal composition process decreases the correlation coefficient for each parameter. Horizontal lines represent 15-year LST composite built without accounting for MODIS QC. Highest correlation coefficient is noted between LST and ISA, second highest between LST and night-time lights and lowest between LST and population density. After applying MODIS QC metadata in the temporal aggregation process, in Spring night case the highest correlation coefficient was noted between LST and night-time lights.

5. Conclusions

The goal of the presented study was to estimate a mean SUHI intensity for a Central-European agglomeration (Warsaw) in transitional seasons (Spring and Autumn). To achieve this goal we analysed the impact of temporal aggregation of LST data on the values of SUHI intensity indicators. The idea of the approach was based on an assumption that according to the nature of thermal remote sensing observations and synoptic conditions over the study area, it can be justified to promote pixels with highest quality. Therefore, we applied a weighted arithmetic mean to calculate the final rasters that represent mean LST values for the period 2000-2014. Weights were accumulated over 15 years and were based on MODIS MOD11A2 Quality Control metadata. We included 3 types of weights, the first based solely on the number of clear-sky days (8 thresholds), the second based on LST retrieval errors (5 thresholds), and the third type a combination of the first and the second type of weights. Moreover, to show the impact of the strength of the promotion of pixels with best quality, we applied 5 exponential powers to weights during the composition process. Also, the differences between 15-year mean rasters built without accounting for MODIS QC metadata and 15-year mean rasters that account for MODIS QC, were discussed.

In Section 4.1 we analysed a spatial distribution of the 15-year mean LST with 5 different exponential powers applied to 3 different types of weights for Spring day cases. We conclude that the combination of weights based on LST retrieval errors and number of clear-sky days gives the most realistic LST pattern. Therefore, this type of composition process was chosen for further analyses. Hence, we analysed a spatial distribution of temporally aggregated LST for day and night, Spring and Autumn cases. We observed that temporal aggregation process does influence the values and spatial range of elevated urban LST.

In Section 4.2 we analysed SUHI intensities in terms of their variability with growing exponential power applied to weights during composition process, as well as differences between temporal composition with and without accounting for MODIS QC. The most important observation is that the SUHI phenomenon occurs in each case analysed. We noted that the temporal aggregation process has a weaker influence on calculated SUHI intensity in Autumn cases than in Spring cases. Moreover, this influence in Autumn cases increases the observed SUHI intensity, while in Spring cases it decreases or increases it, depending on indicator and exponential power. The inclusion of MODIS QC metadata in composition process has the strongest influence on calculated SUHI intensity in Spring night case, since in this case most indicators have bigger differences than indicators calculated on 15-year mean raster built without accounting for MODIS QC. However, we observed that behaviour of SUHI indicators varies. This conclusion is consistent with the findings of Schwarz et al. 2011, where it is remarked that SUHI indicators reveal low correlations between each other.

The conclusion than comes out of analysis of the impact of temporal aggregation of LST data on the relationship between LST and night-time lights, population density and ISA (Section 4.3) is the following. The weakest relationship is observed between LST and population density, while the highest between LST and ISA or night-time lights. Moreover, it is safe to remark that in the Autumn cases, temporal composition process with accounting for MODIS QC brings out the urban LST pattern more apparently (increases correlation) than without accounting for QC metadata. In Spring cases temporal aggregation process suppresses the urban LST pattern (decreases correlation).

References

Buyantuyev, A., & Wu, J. (2009). Urban heat islands and landscape heterogeneity: linking spatiotemporal variations in surface temperatures to land-cover and socioeconomic patterns. *Landscape Ecology*, 25(1), 17–33.

Carlson, T. N., & Traci Arthur, S. (2000). The impact of land use — land cover changes due to urbanization on surface microclimate and hydrology: a satellite perspective. *Global and Planetary Change*, 25(1–2), 49–65.

Clinton, N., & Gong, P. (2013). MODIS detected surface UHI and sinks: Global [...]. *Remote Sens. Environ*., 134, 294–304.

Cui, Y. Y., & de Foy, B. (2012). Seasonal Variations of the Urban Heat Island at the Surface and the Near-Surface and Reductions due to Urban Vegetation in Mexico City. *J. App. Meteo. Clim.,* 51(5), 855–868.

Dousset, B. et al., (2011). Satellite monitoring of summer heat waves in the Paris *[...]. Int. J. Clim*., 31(2), 313–323.

Elvidge, C. D., Baugh, K. E., et al., (1997). Mapping city lights with night-time data from the DMSP operational linescan system. *Photogramm. Eng. Remote Sens*., 63(6), 727–734.

Elvidge, C.D.; Tuttle, B.T. (2007).et al. Global Distribution and Density of Constructed ISA.*Sensors*,*7*, 1962-1979.

Elvidge, C. D., Baugh, K. E., Zhizhin, M., & Hsu, F.-C. (2013). Why VIIRS data are superior to DMSP for mapping nighttime lights. *Proceedings of the Asia-Pacific Advanced Network*, *35*(0), 62–69.

Gallo, K. P., Tarpley, J. D., McNab, A. L., et al.. (1995). Assessment of urban heat islands [...].*Atmos. Res.*, 37(1–3), 37–43

Gawuc, L. (2014). Diurnal variability of SUHI during a heat wave in selected cities in Poland in August 2013 [...]. in: *Scientific Papers of Warsaw University of Technology, Environmental Engineering series*, 68, 19-34

Hu, L.,Brunsell, N. A. (2013). The impact of temporal aggregation of LST[...]. *Remote Sens. Environ*., 134, 162–174.

Jenerette, G. D., Harlan, S. L., Brazel, A., et al., (2006).Regional relationships between surface temperature, vegetation, and human settlement in a rapidly urbanizing ecosystem. *Landscape Ecology*, 22(3), 353–365.

Kato, S.,Yamaguchi, Y. (2005). Analysis of urban heat-island effect using ASTER and ETM+ Data: Separation of anthropogenic heat discharge and natural heat radiation from sensible heat flux. *Remote Sens. Environ*., 99(1–2), 44–54

Li, W., Bai, Y., et al. (2014). Discrepant impacts of land use and land cover on UHI [...]. *Ecological Indicators*, 47, 171–178.

Mallick, J., Rahman, A. (2012). Impact of population density on the surface temperature and micro-climate of Delhi. *Current Science*, 102(12), 1708–1713.

Mohan, M., & Kandya, A. (2015). Impact of urbanization and land-use/land-cover change on diurnal temperature range: A case study of tropical urban airshed of India [...]. *Science of The Total Environ*., 506–507, 453–465.

Quan, J., Chen, Y., Zhan, W., Wang, J., Voogt, J., & Wang, M. (2014). Multi-temporal trajectory of the urban heat island centroid in Beijing, China based on a Gaussian volume model. *Remote Sens. Environ*., 149, 33–46

Roth, M., Oke, T. R., &Emery, W. J. (1989). Satellite-derived urban heat islands from three coastal cities and the utilization of such data in urban climatology. *Int.J. Remote Sens.*, 10(11), 1699–1720.

Schwarz, N., Lautenbach, S., &Seppelt, R. (2011). Exploring indicators for quantifying surface urban heat islands of European cities with MODIS land surface temperatures. *Remote Sens. Environ*., 115(12), 3175–3186

Sharma, R., & Joshi, P. K. (2014). Identifying seasonal heat islands in urban settings of Delhi (India) [...]. *Urb. Clim.*, 9, 19–34.

Stathopoulou, M., &Cartalis, C. (2007). Daytime urban heat islands from Landsat ETM+ and Corine land cover data: An application to major cities in Greece. *Sol. Energy*, 81(3), 358–368

Voogt, J. A., &Oke, T. R. (2003). Thermal remote sensing of urban climates*. Remote Sens. Environ*., 86(3), 370–384.

Wan, Z., (2006).MODIS Land Surface Temperature Products Collection 5 - Users' Guide. ICESS, University of California

Walawender, J. P., Szymanowski, M., Hajto, M. J., & Bokwa, A. (2014).Land Surface Temperature Patterns in the Urban Agglomeration of Krakow (Poland) Derived from Landsat-7/ETM+ Data. *Pure and App. Geophysics*, 171(6), 913–940.

Weng, Q., & Fu, P. (2014). Modeling annual parameters of clear-sky land surface temperature variations and evaluating the impact of cloud cover using time series of Landsat TIR data. *Remote Sens. Environ*., 140, 267–278

Yang, W., Chen, B., & Cui, X. (2014). High-Resolution Mapping of Anthropogenic Heat in China from 1992 to 2010. *Int. J. Environ. Res. and Public Health*, 11(4), 4066–4077.

Yuan, F., & Bauer, M. E. (2007). Comparison of impervious surface area and normalized difference vegetation index as indicators of surface urban heat island effects in Landsat imagery. *Remote Sens. Environ*., 106(3), 375–386.

Zheng, B., Myint, S. W., et al. (2014).Spatial configuration of anthropogenic land [...]. *Landscape Urb. Plann.*, 130, 104–111.

Zhou, Y., Weng, Q., Gurney, K. R, et al., (2012). Estimation of the relationship between remotely sensed anthropogenic heat discharge and building energy use. *ISPRS J. of Photogramm. Remote Sens.*, 67, 65–72.